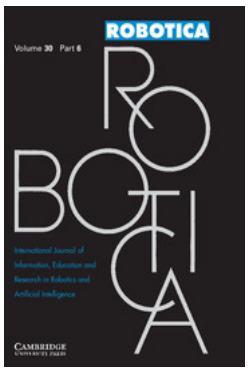

Swimming locomotion modeling for biomimetic underwater vehicle with two undulating long-fins

Liuji Shang, Shuo Wang, Min Tan and Long Cheng

Robotica / Volume 30 / Issue 06 / October 2012, pp 913 - 923
DOI: 10.1017/S0263574711001159, Published online:

Link to this article: http://journals.cambridge.org/abstract_S0263574711001159

How to cite this article:
Liuji Shang, Shuo Wang, Min Tan and Long Cheng (2012). Swimming locomotion modeling for biomimetic underwater vehicle with two undulating long-fins. Robotica,30, pp 913-923 doi:10.1017/S0263574711001159

Robotica (2012) volume 30, pp. 913–923. © Cambridge University Press 2011
doi:10.1017/S0263574711001159

Swimming locomotion modeling for biomimetic underwater vehicle with two undulating long-fins

Liuji Shang, Shuo Wang*, Min Tan, Long Cheng

State Key Laboratory of Intelligent Control and Management of Complex Systems, Institute of Automation, Chinese Academy of Sciences, 95 Zhongguancun East Road, Beijing 100190, China

(Accepted September 29, 2011. First published online: November 1, 2011)

SUMMARY

A biomimetic underwater vehicle, which is propelled by two undulating long-fins, is introduced in this paper. The undulating or oscillating movements of symmetrical long-fins cause the complex locomotion of biomimetic underwater vehicle. For convenience, three motion modes are proposed and considered firstly. Then an inertial unit is installed for collection of accelerations and angular velocity. The underwater vehicle's MIMO model is reduced into a SISO model by some simplifications. A sine wave function deduced from the long-fin's time-varying membrane is proposed and used as the input of the biomimetic underwater vehicle ARMA model, and velocity or angular velocity is considered as the model output. The algorithms based on recursive weighted least squares are applied for model parameter identification. Experiments carried out with a long-fin propelled underwater vehicle. The experimental results show that the proposed methods can build valid locomotion models for three motion modes efficiently.

KEYWORDS: Biomimetic underwater vehicle; Recursive weighted least squares; Modeling; Parameter identification.

1. Introduction

Research on biomimetic underwater robots is driven by the demand of applications and fitness in complex underwater circumstances. Presently, complicated operations in dangerous environments make traditional autonomous underwater vehicles (AUV) incompetent on autonomous ability and hydrodynamic efficiency. Due to increasing demand in terms of high efficiency propulsion, robustness and long work duration, considerable research has been conducted on AUV, especially in the field of biomimetic underwater robots. Fishes exist in oceans for thousands of years. Although their architecture may not be optimal, fishes have some special characteristics, such as pre-eminent flexibility, excellent maneuverability, durative cruising ability, etc.[1] These characteristics inspire a new design idea for AUV. In addition, compared with traditional underwater vehicles, low-noise propulsion and less significant trail of fishes are also very remarkable, especially in military applications. Therefore, many researchers have focused on design and hydrodynamic analysis of biomimetic underwater vehicles (BUV). On account of its significance in practical applications, fish-like underwater vehicles with excellent maneuverability can fulfill many particular underwater jobs, for example oceanic supervision, pollution detection, surveillance and reconnaissance, and so forth.[2] But the modeling and control of this new kind of biomimetic vehicles are still ongoing and not mature for practical applications.

Generally speaking, fish propulsion systems can be divided into (1) median and paired fin (MPF) propulsion; and (2) body and caudal fin (BCF) propulsion.[3] Almost all BUV prototypes are designed to mimic the structure of natural fishes. Compared with BCF propulsion, MPF propulsion has a high maneuverability in the low-speed swimming mode. Especially in the complex turbulent environment, it has higher efficiency, better stability and better capacity of counteracting disturbances than BCF propulsion.[4] Therefore, it is more suitable in adjacent seas. In recent years, researchers have begun to work on MPF propulsion such as *Chaetodon Spp, Gymnarchus Niloticus, Notopterus Chitara*, and so forth.[5]

The BUV in this paper employs an MPF propulsion system. It has two completely symmetric long-fins installed on the vehicle's body. The Field-Programmable Gate-Array (FPGA)-based driving board drives 10 servo motors composed of the long-fin on each side long-fin. One inertial sensor unit (labeled 3DM-GX1), which has three accelerometers, three magnetometers and three gyroscopes, is used to collect inertial data. Another embedded board with ARM-Linux system receives the inertial sensor data and processes these into certain information as needed.

Based on hydrodynamic analysis and special mechanism, our fish-like underwater vehicle can generate three motion modes: marching mode, receding mode and rotating mode. It is obvious that most of the common locomotion can be achieved through a combination of these three motion modes. Hydrodynamic analysis may be simplified to a great extent by dividing the underwater vehicle locomotion into three parts. The instantaneous velocity is concerned with marching and receding modes. The same applies to the rotating mode with instantaneous angular velocity concerned. Then a special

* Corresponding author. E-mail: shuo.wang@ia.ac.cn
This work was supported in part by the National Natural Science Foundation of China Grants 51175496, 60725309, and 61004099, and in part by the National High Technology Research.

method is adopted, which uses the oscillating waveform of fin-ray as the system input of vehicle system instead of complex multi-input of 20 servo-motors. A function defined by the oscillating discipline of the fin-ray is considered as input variables, which fuses physical significance of servo-motors. Therefore, vehicle system is transformed into a single input and single output (SISO) system. Then, the recursive weighted least squares (RWLS) identification algorithm is employed for modeling different modes. More satisfying control algorithms can be applied by these locomotion models.

The remainder of this paper is organized as follows. A brief literature review on biomimetic underwater robots is introduced in Section 2. Section 3 introduces the BUV prototype and proposes three motion modes. Section 4 presents the modeling algorithm based on the RWLS identification. The sensor data collection and processing for modeling of the vehicle are described in Section 5. Section 6 shows the experimental results and corresponding discussions. At last, conclusions are given in Section 7.

2. Related Work

The MPF propulsion system consists of median or paired fins and can be classified into amiiform, gymnotiform, balistform and rajiform according to different propulsive types. For amiiform and gymnotiform locomotions, the whole body participates in undulation and it may achieve receding mode by reversing the angular velocity with mirror-image symmetrical configuration body.[6] Balistform fish has rigid body and its locomotion depends on soft dorsal fin and anal fin. In rajiform locomotion, fish body does not participate in undulation and only the two long-fins do sorts of undulating.[7] Compared with the other three kinds of fishes, rajiform fish has symmetrical architecture and propulsive fins, which provide it more excellent maneuverability to be considered as a reference for AUV working in turbulent environments. In addition, rajiform fish has a stable body, which does not participate in undulation and is more convenient for engineering realization.

Hydrodynamic analysis and observation data processing are two important tools to study the fish-like locomotion. Lots of fundamental theoretical studies have been done for applying MPF propulsion. In the early research, Lighthill[8] proposed the elongated body theory,which was based on how swimming modes were produced. By applying to the elongated body theory, the large-amplitude elongated body theory[9] can deal with propulsion performance analysis of soft long-fin undulating propulsion. Blake developed an actuator-disc theory,[10] which is a special application of momentum theorem in hydrokinetics. Its basic idea was simplifying propulsion architecture as an ideal actuator-disc and thrust was obtained by integrating water pressure increment for the whole actuator-disc area. Wu proposed the two-dimensional waving plate theory[11] and treated the robotic fish as an elastic elongated thin plate. Daniel[12] proposed the waving plate theory, which was extended by blade element analysis method and used it for swimming performance analysis of rajiform. All these works provided a basic theory support for the fish-like BUV.

Based on theory analysis, many artificial robotic fishes are developed to analyze and implement MPF propulsion. Sfakiotakis *et al.*[13] at Heriot-Watt University developed the earliest undulating-fin device using parallel bellows actuator. It used elastic material to build long-fin and parallel bellows actuator to drive long-fin. Epstein *et al.*[14] at Northwestern University designed a bio-inspired robotic ribbon fin, which used eight servo motors to drive the long-fin. Shen *et al.*[5] at National University of Defense Technology designed a BUV to mimic *Gymnarchus Niloticus*. Osaka University in Japan and Nanyang Technological University in Singapore respectively proposed two robotic rajiform fishes, which have two soft elastic long-fins and a rigid body.[15,16] Hydrodynamic analysis was used to model robotic fishes based on their unique mechanical architecture. Jennie *et al.*[17] analyzed the hydrodynamic force generated by the fish's oscillating body in water. They modeled robotic fish based on "vortex shedding". Yu *et al.*[18] proposed a dynamic modeling method by integrating hydrodynamic force in three parts of robotic fish. Low and Willy[19] proposed a modeling method based on simplifying two adjacent fin-rays as 2-degree-of-freedom (DOF) mechanisms. MacIver *et al.*,[20] proposed an idealized ellipsoidal body modeling method based on Kirchhoff's equations, which treated robotic fish as a rigid ellipsoid. Cheng *et al.*[21] proposed a modeling algorithm by merging elongated body theory and hybrid tail dynamics. Zhang[22] proposed a modeling algorithm for three-layer structure motors for robotic fish. Transeth *et al.*[23] given a summary on modeling method of snake-like robot. Earlier, a modeling algorithm based on the three-dimensional waving plate theory was proposed by Cheng *et al*.[24]

These researches on theoretical analysis, design and modeling have a great impact on the development of MPF propulsion. However, there is still a lot of work to do, especially on modeling of BUV control in navigation, path following, disturbance rejection, etc. As mentioned above, most of the model analysis assume that the robotic fish works is ideal fluid. Obviously, this assumption is realistic. Another issue is that there are too many approximations in analyzing hydrodynamic force because the hydrodynamic analysis is indeed complicated for each underwater robot prototype. In addition, the characteristics of underwater robot may change because of some external factors. Therefore, it is necessary to find a modeling method that may be valid for BUV in turbulent non-ideal fluid. The contribution of this paper lies in the following: (1) A BUV prototype is designed, then three motion modes are implemented by using different control methods of symmetrical long-fins; and (2) it proposes a modeling algorithm based on the parameter identification method for BUV. With suitable simplification, the given algorithm can be used further for online modeling. In addition, most of the researches on BUV focus on fish-like propulsion, but seldom address the importance of real-time modeling and control for BUV working in a complex environment. The data processing and modeling methods based on inertial sensors in this paper are significant for BUV to enhance their abilities such as navigation, path-following, disturbance rejection, etc.

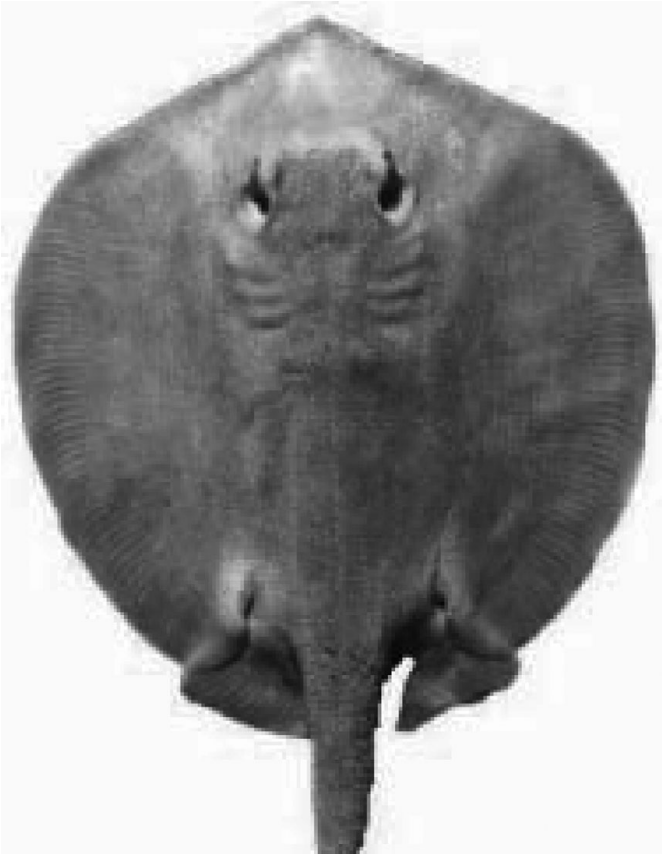

Fig. 1. Taeniura lymma.

3. Biomimetic Vehicle Prototype and Motion Modes

3.1. Biomimetic vehicle prototype

Taeniura lymma shown in Fig. 1 is a kind of Dasyatidae fish in the Pacific.[25] Its propulsion system depends on two symmetrical bilateral fins. There are a lot of fin-rays in the long-fins. The fin-rays oscillate at different frequencies and amplitude, which drive the two long-fins into different waveforms to produce hydrodynamic force. According to this idea our BUV prototype is designed. Without caudal and pelvic fins, the underwater vehicle prototype has only two symmetrical long-fins on the sides of its body. Figure 2 shows its prototype.

The prototype body is made of glass fiber reinforced plastic. Instead of biological fin-rays, the prototype system employs 10 equally distributed thin rigid rods installed on both sides.[26] A soft elastic flat membrane is covered on 10 fin-rays, and one servo motor is installed at the end of each fin-ray. The signal input of servo motor is controlled by driving system based on FPGA. The prototype system oscillates 10 fin-rays on both sides and makes the membrane bend at some waveform when it swims in water.

3.2. Three motion modes

Based on the special system architecture, three basic motion modes can be achieved, which includes marching mode, receding mode and rotating mode.[26]

If hydrodynamic force on both sides of the vehicle has same magnitude and same heading direction, forward marching can be generated according to hydrodynamic

Fig. 2. Our vehicle prototype.

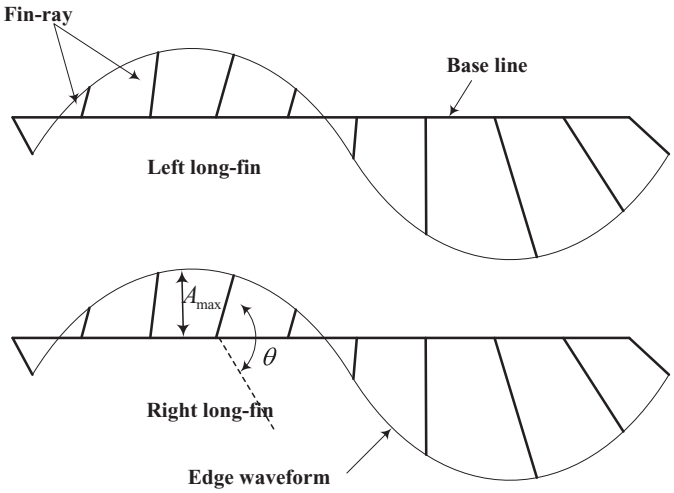

Fig. 3. Long-fins shape in marching mode.

analysis. With kinematic analysis of real fish, fin-ray control based on sine function is adopted. Define the edge waveform function of the membrane as ϕ, the amplitude as $A_{\max}$ and the oscillating frequency as f. The immediate phase is φ. Then,

$$\phi = A_{\max} \sin(2\pi f t + \varphi). \tag{1}$$

Equation (1) shows the oscillating discipline of every fin-ray, and there exists specific phase difference θ between adjacent fin-rays. Figure 3 shows the long-fins shape in marching mode.

Obviously, if servo motors on both sides are applied the same control signals, then the same heading traveling waveform on the membranes can be generated. As a result, the thrust on both sides is same and symmetrical, which means marching mode is generated. Another important point is that different oscillating frequencies and amplitude of membranes' waveform decide relevant hydrodynamic force to propel the vehicle. Similar to the marching mode, receding mode is produced by controlling servo motors on both

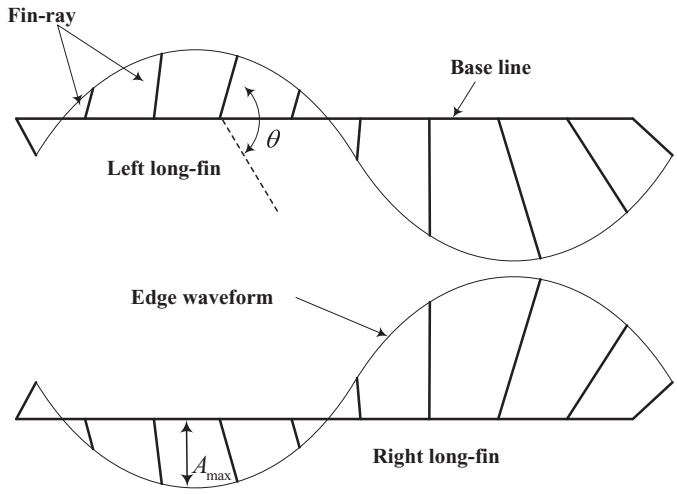

Fig. 4. Long-fins shape in rotating mode.

sides to generate same backward traveling waveform on membranes.

The third motion mode is rotating mode. In a similar way if the control signals of servo motors on both sides are reversed to generate opposite traveling waveform on the membranes, hydrodynamic forces may cause a rotary moment and make the vehicle rotate. Figure 4 shows long-fins shape in rotating mode.

In rotating mode, the waveform on two long fins' membranes has same oscillating amplitude and frequency, but are in anti-phase. The anti-phase undulating long-fins generate opposite thrust to make the vehicle rotate, and Eq. (2) shows the oscillating discipline in rotating mode. ϕ_L and ϕ_R are the edge waveform functions of the membrane for the left long-fin and right long-fin, respectively.

$$\begin{aligned} \phi_L &= A_{\max} \sin(2\pi f t + \varphi), \\ \phi_R &= -A_{\max} \sin(2\pi f t + \varphi). \end{aligned} \tag{2}$$

The three motion modes are the basic motion modes for the vehicle with two long-fins. More locomotion modes may be achieved by adjusting the oscillating amplitude, frequency and phase difference of two long-fins.

4. Simplification and Modeling for the Vehicle

Modeling is important for BUV in navigation and locomotion control. Traditionally, hydrodynamic analysis is used for underwater robotic robots modeling.[27,28] But it is not suitable for our vehicle prototype because of two reasons. One is that hydrodynamic analysis for undulating long-fins in turbulent fluid is too complicated. Another is locomotion diversity of the vehicle generating different waveforms on the membranes by 10 rotating rods on each side. The vehicle with undulating long-fins is a nonlinear multi-input multi-output (MIMO) system. In practical applications, there always exist uncertain disturbances or unexpected situations such as mechanism damage or change and turbulence, so an online model identification algorithm does more help to navigation and motion control of the vehicle. In this paper, a special method is proposed to simplify the underwater vehicle modeling. Based on simplification, the RWLS algorithm is employed.

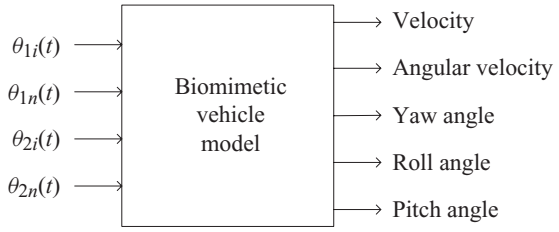

Fig. 5. Nonlinear MIMO model for the vehicle.

4.1. Model simplification and model establishment

Generally speaking, the vehicle introduced in this paper is a nonlinear MIMO system. As shown in Fig. 5, $\theta_{1i}(t)$ is the rotating angle of the ith rod servo motor on one side of the vehicle and $\theta_{2i}(t)$ is the angular of the ith rod servo motor on the other side of the vehicle. The rotating angles of the servo motors on each side are coupled because of the membrane. The inputs of the system are rotating angles of rods' servo motors, and the outputs include velocity, angular velocity, yaw angle, roll angle and pitch angle, as shown in Fig. 5.

For the convenience of analysis, the following parts focus on three basic motion modes proposed in the above section. For the purpose of generating waveform shown in Eqs. (1) and (2), the rotating motion of each rod on one side is in accordance with sine function with special frequency, amplitude and phase difference. And for marching and receding modes, angular velocity, yaw angle and so forth are not concerned and the special concerned output variable is instantaneous velocity. In rotating mode, angular velocity is the special concerned output variable. So the multi-output of the vehicle model is simplified into one-output for each special motion mode.

Another issue of the model is the multi-input variables. As mentioned above, servo motors of the vehicle are driven on the basis of sine wave control discipline, which is an effective and experiment-tested driving method. On the developed vehicle, 20 servo motors are installed and oscillating motion of each rod servo motor needs three parameters: oscillating frequency, amplitude and phase difference. Obviously, it is hard to model the vehicle with these coupled input variables. Hence, a method reducing inputs based on former analysis is presented. For the vehicle, length of fin-ray and distance between adjacent fin-rays are constant, and control signals of the servo motor make the rod oscillating and every fin-ray adopts similar oscillating rules. The oscillating rods generate traveling waveform of different frequencies and amplitude on the membranes to produce different motion mode. So, 60 input parameters of the vehicle are reduced to the oscillating frequency and amplitude of the first fin-ray, whose motion has same oscillating frequency and similar amplitude as the waveform on the membranes. Here a function output is used to substitute input variables. Equation (3) shows the substitute function:

$$F_u = A \sin(2\pi f t) + \varepsilon, \tag{3}$$

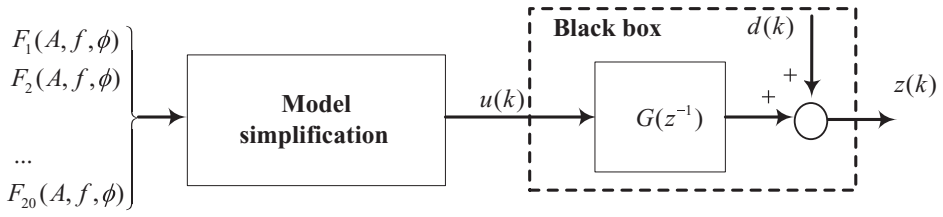

Fig. 6. Identification diagram.

where F_u is the input variable for model identification, A and f are the oscillating amplitude and frequency of servo motors, respectively. ε means white noise signals for system input and its mathematical expectation is zero. In this way, F_u also reflects physical characteristics of servo motors and is workable for identification.

With the methods mentioned above, robotic fish may be regarded as a SISO system. Normally, the system is considered as a black box structure and the corresponding identification diagram is shown in Fig. 6.

Here, $F_k(A, f, \phi)(k = 1, 2, \ldots, 20)$ is the oscillating function for the kth fin-ray, and $u(k)$ and $z(k)$ correspond to input variable F_u and output variable, respectively. $G(z^{-1})$ represents the vehicle system. $d(k)$ is system disturbance. The identification method only studies the input–output relationship rather than the essential mechanism principle. Generally, $G(z^{-1})$ is used to describe the input–output relationship and always be expressed as

$$G(z^{-1}) = B(z^{-1})/A(z^{-1}), \tag{4}$$

where

$$\begin{cases} A(z^{-1}) = 1 + a_1 z^{-1} + a_2 z^{-2} + \cdots + a_n z^{-n} \\ B(z^{-1}) = b_1 z^{-1} + b_2 z^{-2} + \cdots + b_m z^{-m} \end{cases}, \tag{5}$$

n is the order of the system model.

4.2. Recursive weighted least squares (RWLS) algorithm

The online model identification algorithm for the vehicle, which may be run in an embedded board, should be effective and accurate. For normal fish-like underwater vehicles, which have limited computational capabilities, an online traditional least squares identification is suitable. So a modified identification algorithm based on least squares is employed in this paper, which is called recursive weighted least squares model identification algorithm.

The RWLS algorithm is an online recursive algorithm based on the following mathematical model:

$$A(z^{-1})z(k) = B(z^{-1})u(k) + d(k). \tag{6}$$

Its basic idea is that the estimated unknown parameters are updated according to new observation data. Another important element is the weight coefficient Λ, which stands for the trust degree to unknown parameters last time. The bigger the weight coefficient, the bigger the confidence coefficient it has, and *vice versa*.

In this paper, inputs $u(k)(k = 0, 1, 2, \ldots\ (F_u))$ and outputs $z(k)(k = 0, 1, 2, \ldots)$ are accessible at each sampling time k. By defining the unknown parameters vector as θ, the information vector $h(k)$ can be described as

$$\begin{cases} \theta = [a_1, a_2, \cdots, a_n, b_1, b_2, \ldots, b_m] \\ h(k) = [-z(k-1), \ldots, -z(k-n), \\ \quad u(k-1), \ldots, u(k-m)]^T \end{cases}. \tag{7}$$

Then, Eq. (6) can be rewritten in the following compact form:

$$z(k) = h^T(k)\theta + d(k). \tag{8}$$

Based on the least squares algorithm, the RWLS model identification algorithm can be described by the following equations:

$$\begin{cases} \theta(k) = \theta(k-1) + K(k)[z(k) - h^T(k)\theta(k-1)] \\ K(k) = P(k-1)h(k)[h^T(k)P(k-1)h(k) + 1/\Lambda]^{-1} \\ P(k) = [I - K(k)h^T]P(k-1) \end{cases}, \tag{9}$$

where $K(k)$ is the gain matrix and I is the identity matrix. $P(k-1)$ is the symmetric matrix with an initial value $a^2 I$ (a is a positive integer, usually bigger than 10^3). The initial value of unknown parameter vector may be choosen to be a small real number (less than 10^{-3}).

The RWLS algorithm is easier to be realized and it needs less memory for embedded board. Thus, it also ensures that we can identify the model of robotic fish online. Experiments on vehicle prototype show the validity of the proposed method.

5. Preprocessing of Sensor Data

5.1. Data collection platform

Different from traditional small-size, fish-like underwater vehicles, our vehicle prototype has a large body. As shown in Fig. 2, a vehicle with two long-fins separates the servo motors from fish body and it also has enough space to install sensors. Therefore, a data collection platform could be built and Fig. 7 shows the internal structure inside the robotic vehicle.

In Fig. 7, a 3DM-GX1 sensor made by MicroStrain is used for data collection. There are three accelerometers, magnetometers and gyroscopes each inside 3DM-GX1. Its data communication protocol is based on RS-485 and the sensor data can be obtained from a serial port. Sampling frequency of 3DM-GX1 can reach up to 350 Hz. Table I shows the important specifications of 3DM-GX1.

A control board installed with ARM-Linux system is employed for data processing, online modeling and real-time

Table I. Specifications of 3DM-GX1.

	Parameter	Specification
Pose	Dynamic accuracy (°rms)	+/−2
Acceleration	Short-term stability (mg)	0.2
Angular Rate	Angle random walk, noise (°/h)	3.5
Sampling	Maximum frequency (Hz)	350

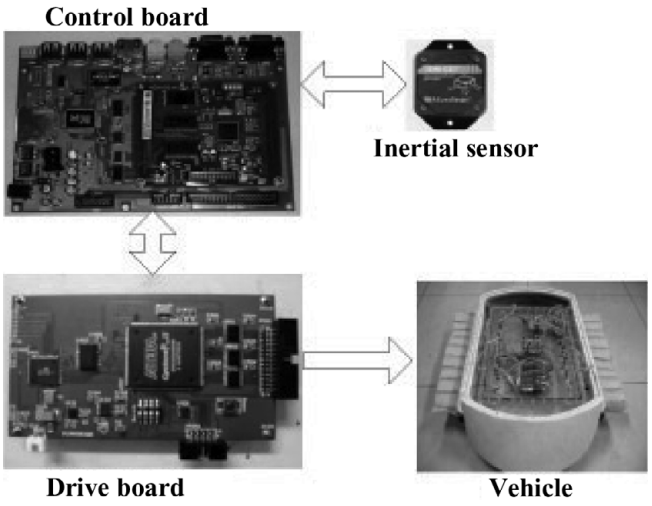

Fig. 7. Internal structure of vehicle.

control. The control board receives sensing data from 3DM-GX1 sensor. These sensing data are raw data and should be changed into the needed information. The drive board is designed to drive 20 servo motors to propel the vehicle.

5.2. Sensor data processing

Previously, a 3DM-GX1 inertial sensor was employed to collect vehicle information. These raw data are processed into the needed data format where the instantaneous acceleration and instantaneous angular velocity on three axes are included. In addition, the quaternion of vehicle could also be achieved through a filtering algorithm embedded in 3DM-GX1. Quaternion is often used for calculating the pose of aerial objects. Two data process strategies are given to decrease the effect of above issues.

As well known, there are two crucial issues for inertial sensors. One is that they are very sensitive to external disturbances, especially vibration disturbances. The other is the accumulated error caused by drift and calibrated errors that may be increased with the lapse of time. Here data processing algorithm uses two steps to deal with errors. First, for each motion mode, a filtering DC component method is used. Second, for inhibiting static error, which is small and not very clear, a threshold value is set. The sensor data whose absolute value is less than the threshold value are discarded.

Through data processing, roll-pitch-yaw of the vehicle may be directly measured by inertial measurement unit (IMU).

5.3. Instantaneous velocity and instantaneous position

Sensor data, including instantaneous acceleration and angular velocity, are obtained based on the vehicle coordinate system. As model identification needs acceleration in the earth coordinate system, transformation needs to be done. By defining the acceleration as a, Eq. (10) describes the transformation as

$$a_e = \left(M_e^f\right)^{-1} * a_f. \tag{10}$$

In the same way, angular velocity ω can also be obtained by Eq. (11):

$$\omega_e = \left(M_e^f\right)^{-1} * \omega_f. \tag{11}$$

Then, instantaneous velocity of the vehicle can be calculated by an integrative approach. In a discrete computer control system, an approximation method is used to get the

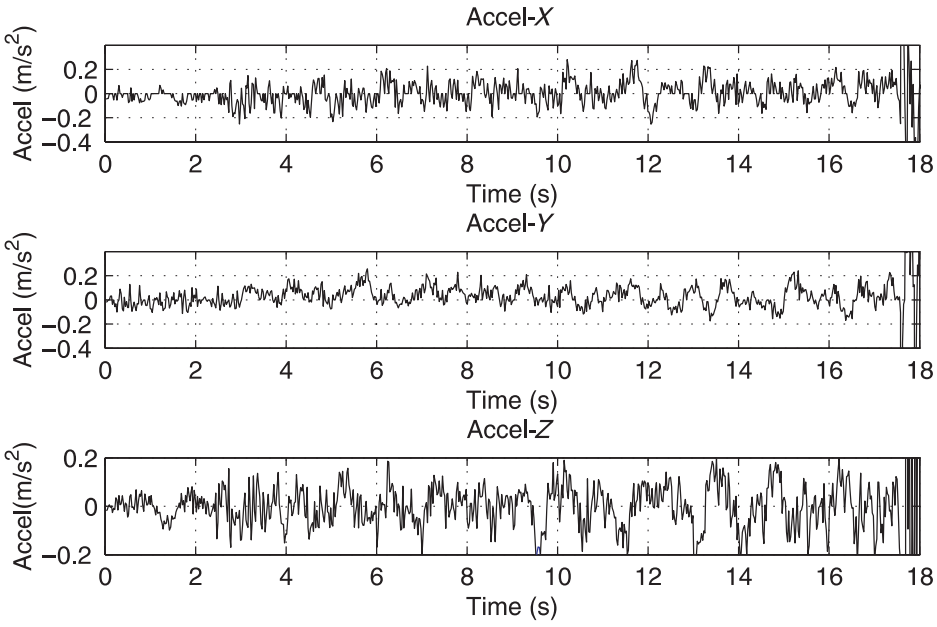

Fig. 8. (Colour online) Instantaneous acceleration on three axes.

Table II. Parameters identification result in marching mode.

Parameter	a_1	a_2	a_3	a_4	b_1	b_2	b_3
$m = 2, n = 3, \Lambda = 0.93$	-1.921	1.069	-0.147		-2.278×10^{-3}	2.695×10^{-3}	
$m = 3, n = 4, \Lambda = 0.95$	-2.023	1.489	-0.815	0.350	1.140×10^{-4}	2.881×10^{-4}	6.670×10^{-4}

velocity as follows:

$$v(i) = \int_0^i a(t)dt \approx \sum_0^i (a(i) + a(i-1))/2 * \triangle t, \quad (12)$$

where i means sampling moment, and $\triangle t$ means sampling interval. In the sequel, the same method is used for position by reference P for robotic fish. Through integrating velocity, positioning algorithm may be expressed as follows:

$$P(i) = P\ (i-1) + \int_{i-1}^i v(t)dt \approx P\ (i-1) + (v(i) + v(i-1))/2 * \triangle t. \quad (13)$$

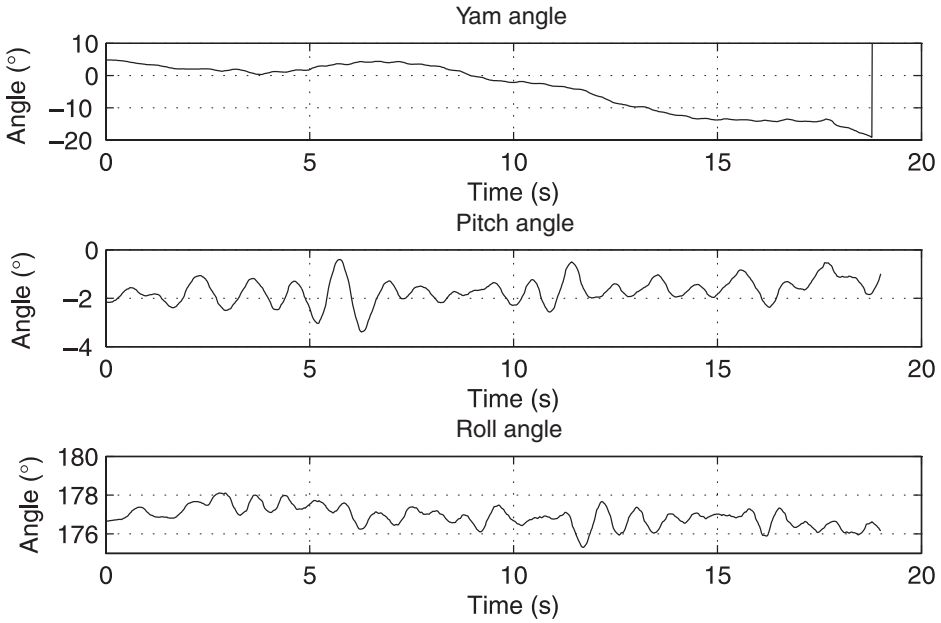

Fig. 9. Instantaneous pose on three axes.

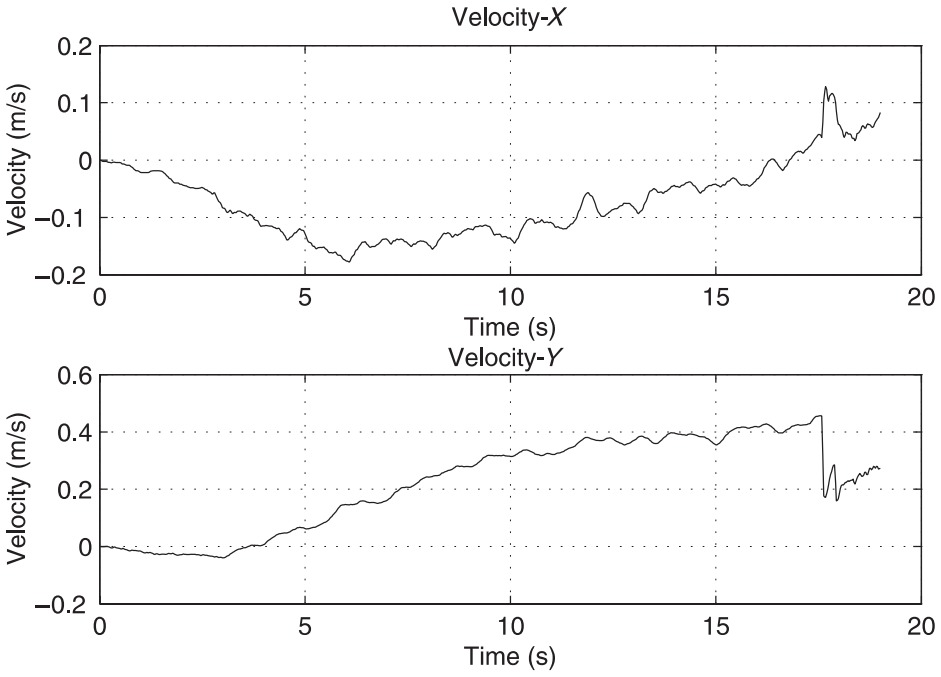

Fig. 10. Instantaneous velocity on two axes.

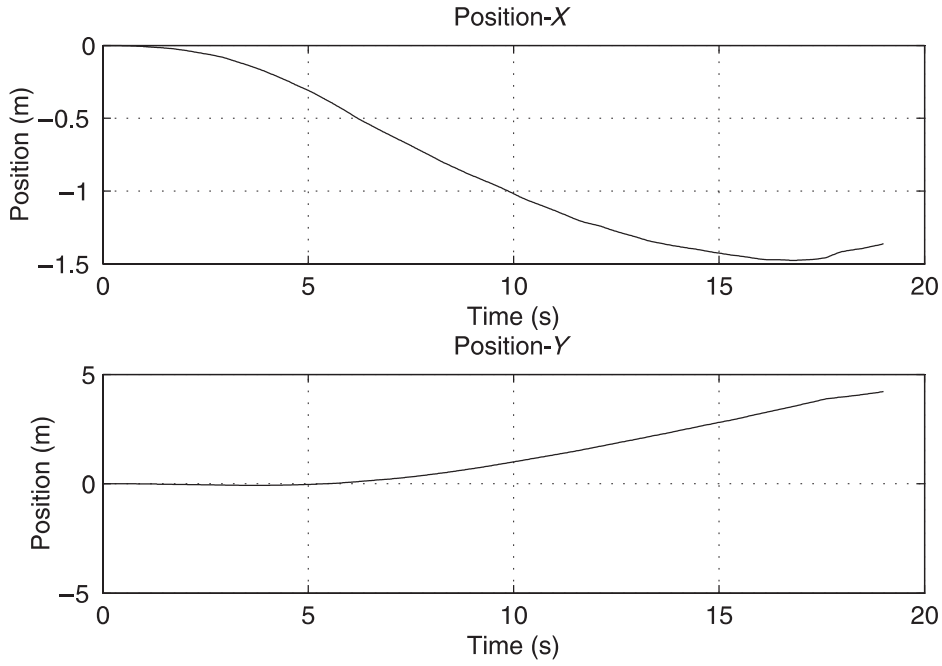

Fig. 11. Instantaneous position on two axes.

Positioning algorithm processes filter and supply sensor data for model identification algorithm, including velocity and angular velocity for model parameter identification. For the vehicle without strenuous vibration and high acceleration, the integrative approach has high accuracy and is acceptable.

6. Experiments and Analysis

The experiments are divided into two parts. One is the velocity model identification experiments, including marching and receding modes. Another is the angular model identification experiments, including rotating mode. In the experiments, IMU sensors, including 3DM-GX1, are used to collect inertial information and the methods mentioned above are used to compute the instantaneous pose, velocity or angular velocity of the vehicle. For each experiment's part, experimental results are given and analyzed.

6.1. Velocity model identification experiments

For marching and receding modes, the output concerned is velocity. The method proposed in the paper is applied to model the vehicle in marching mode.

First, positioning algorithm is used in the marching mode experiment. Experiment lasted for 18 s and the sampling period was 0.02375 s. The preprocessed acceleration data of vehicle on three axes are shown in Fig. 8.

Then the positioning algorithm in Section 2 was used to calculate instantaneous pose, position and velocity of robotic fish. Figures 9–11 show the experimental results. After 18 s, experiments were stopped by experimenters but the IMU was still working. Therefore, there was a sudden surging/drop on the curve at the end.

The vehicle in the marching mode has no displacement on Z-axis. In Fig. 9, pitch and roll angles are almost maintained in a small range. It corresponds with the real pose of robotic fish and also proves that the data processing and pose

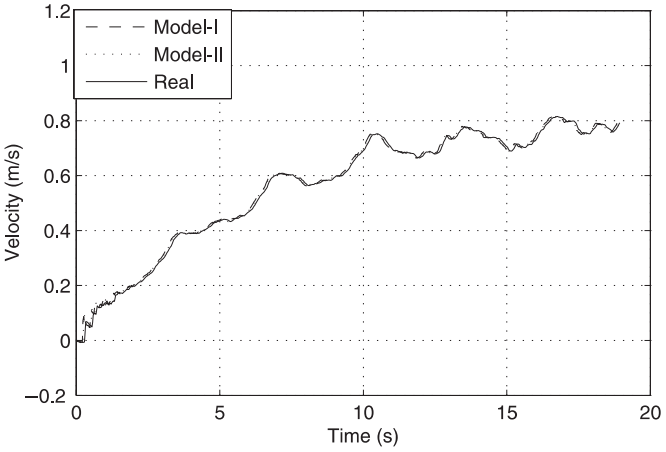

Fig. 12. Marching model verification.

algorithm are valid. Figures 10 and 11 show that there are velocity and displacement on X-axis. Two important factors cause the displacement. One is the initial installation error of 3DM-GX1. The other is uncertain disturbances in marching mode, such as center-of-gravity shift and water wave. This does not reflect the identification algorithm because the velocities on three axes are also obtained.

Then the RWLS identification algorithm is executed twice. Two groups of different weight coefficients and orders are chosen, (1) $m = 2, n = 3, \Lambda = 0.93$; (2) $m = 3, n = 4, \Lambda = 0.95$. The RWLS algorithm uses 534 group data for identification and another complete experiment, which includes 800 group data for model verification. The identification results for unknown parameter θ are listed in Table II.

Based on the identification model listed above, another experiment, which changes inputs, is carried out to verify the model. After data processing, velocity data are sent to our two identification models and the verification results are shown in Fig. 12.

Table III. Parameters identification result in rotating mode.

Parameter	a_1	a_2	a_3	a_4	b_1	b_2	b_3
$m = 3, n = 4, \Lambda = 0.95$	−0.462	−0.460	−0.162	0.082	-4.467×10^{-3}	-6.193×10^{-3}	-6.410×10^{-3}

Figure 12 shows that model identification based on the RWLS algorithm in marching mode for our vehicle has fairly high accuracy.

6.2. Angular velocity model identification experiments

Different from marching mode, angular velocity is concerned in rotating mode. Angular velocity model identification experiment lasts for 28 s and sampling period is 0.0533 s. As oscillating period of long-fin is in the range of 0.67 to 1 s, it satisfies Shannon's sampling theorem and can be used for model identification. The data of the first 21 s are used for parameter identification and that of the last 7 s are used for model verification. The instantaneous pose and instantaneous angular velocity on three axes are also calculated and shown in Figs. 13 and 14, respectively.

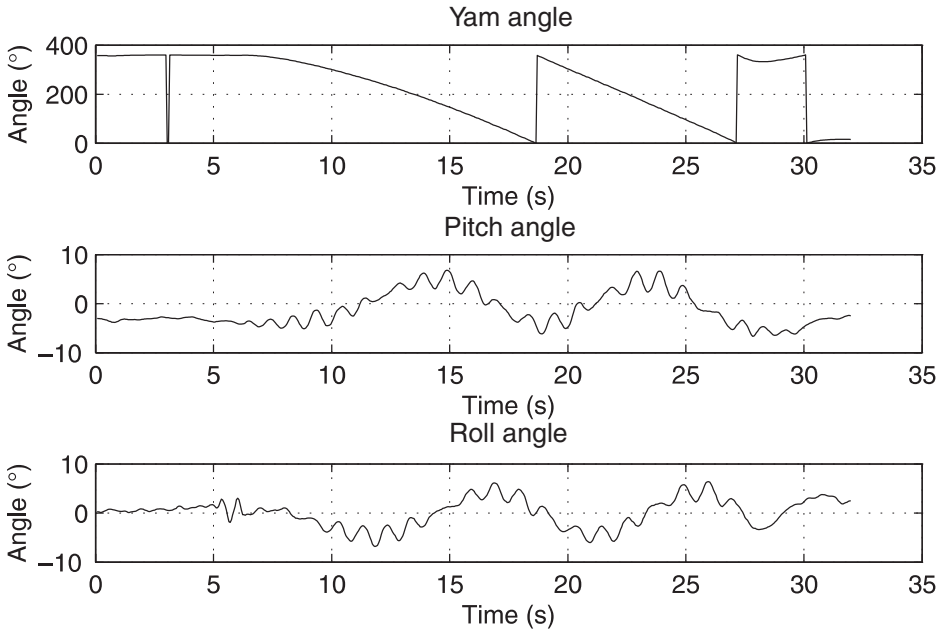

Fig. 13. Instantaneous pose in rotating mode.

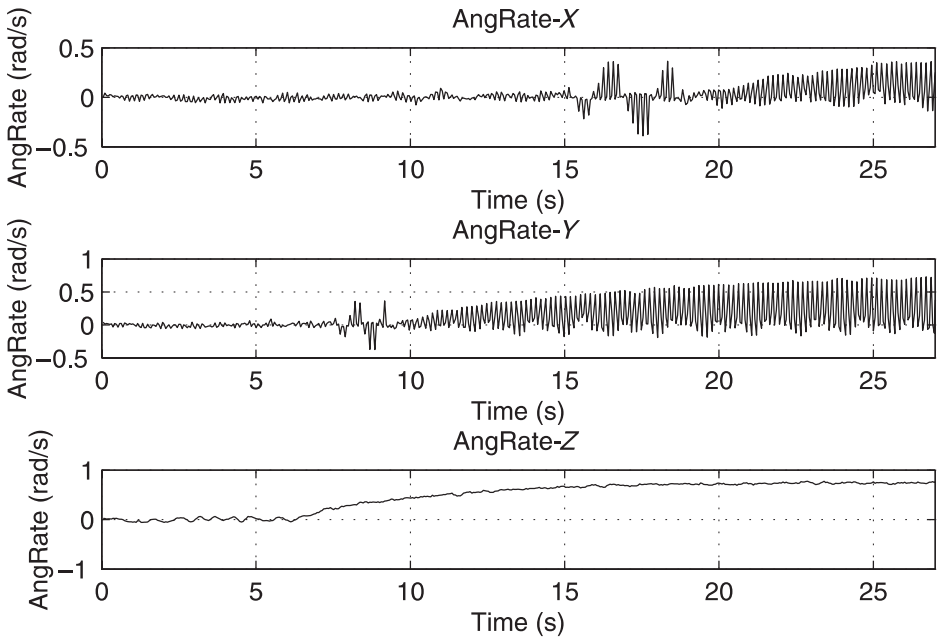

Fig. 14. Instantaneous angular velocity on three axes.

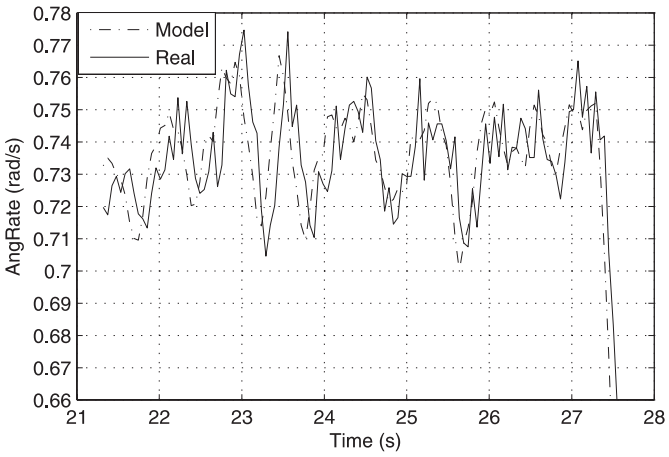

Fig. 15. Rotating model verification.

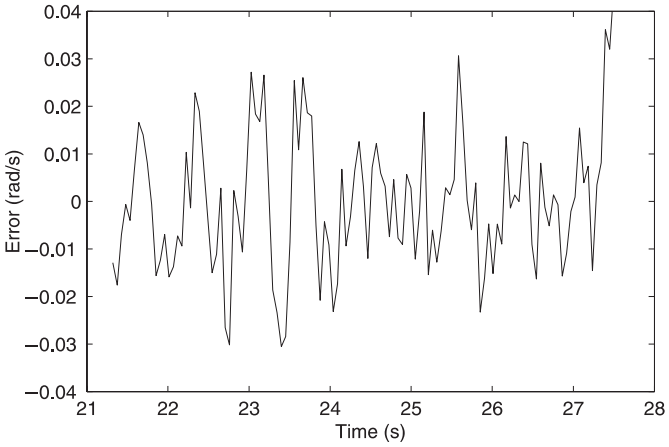

Fig. 16. Model verification error.

Similar to velocity model identification process, the RWLS algorithm is used for model parameter identification in rotating model. Here 390 group data are used for identification and another 130 for model verification. Defining $m = 3, n = 4, \Lambda = 0.95$, identification result for unknown parameter θ is shown in Table III.

The model verification results are shown in Figs. 15 and 16.

Figure 16 shows the identification error in rotating mode, which exists in $[-0.03, 0.03]$ and satisfies control demands in real applications.

The two parameter identification experiments mentioned above show that the method proposed in this paper is satisfactory for our BUV modeling. Each model is built for each BUV motion mode. It shows that this method may fit the true system well and has very high identification accuracy.

7. Conclusions

In this paper, locomotion modeling is considered for a novel BUV propelled by symmetrically installed long-fins. The proposed method in the paper is used to reduce the BUV MIMO model into a SISO model, and a model parameter identification algorithm is applied. The proposed method is valid and efficient, but only considered for three special locomotion modes of the underwater vehicle. Therefore, the model structure could be improved in the future to fit the complex locomotion on-line modeling of the BUV. The BUV real-time controller will also be considered on the basis of system modeling.

Acknowledgment

The authors would like to thank the referees for their careful reading of the manuscript and helpful comments.

References

1. G. Drucker and G. V. Lauder, "Locomotor function of the dorsal fin in rainbow trout: Kinematics patterns and hydrodynamic forces," *J. Exp. Biol.* **208**, 4479–4494 (2005).
2. G. V. Lauder and E. D. Tytell, "Hydrodynamics of undulatory propulsion," *Fish Biomech.* **23**, 425–468 (2006).
3. Y. Toda, N. Sogihara, Y. Sanada and M. Danno, "The Motion of a Fish-Like Under-Water Vehicle with Two Undulating Side Fins," *Proceedings of the International Symposium on Aero Aqua Bio-Mechanisms* (July 2006).
4. P. W. Webb, *The Biology of Fish Swimming* (Cambridge University Press, Cambridge, UK, 1994).
5. T. Hu, L. C. Shen, L. Lin and H. Hu, "Biological inspirations, kinematics modeling, mechanism design and experiments on an undulating robotic fin inspired by Gymnarchus niloticus," *Mech. Mach. Theory* **44**, 633–645 (2009).
6. M. J. Lighthill and R. W. Blake, "Biofluid dynamics of balistiform and gymnotiform locomotion. Part 1. Biological background, and analysis by elongated-body theory," *J. Fluid Mech.* **212**, 183–207 (1990).
7. J. J. Videler, *Fish Swimming* (Chapman and Hall, London, 1993).
8. M. J. Lighthill, "Note on the swimming of slender sh," *J. Fluid Mech.* **9**, 305–317 (1960).
9. J. Y. Cheng and R. Blickhan, "Note on the calculation of propeller efficiency using elongated body theory," *J. Exp. Biol.* **192**, 169–177 (1994).
10. R. W. Blake, *Median and Paired Fin Propulsion, Fish Biomechanics* (Praeger, New York, 1983).
11. T. Y. Wu, "Swimming of a waving plate," *J. Fluid Mech.* **10**, 321–344 (1961).
12. T. Daniel, "Forword flapping flight from flexible fins," *Can. J. Zool.* **66**, 630–638 (1988).
13. M. Sfakiotakis, D. M. Lane and B. C. Davies, "An Experimental Undulating-Fin Device Using the Parallel Bellows Actuator," **In**: *Proceedings of the International Conference Robotics and Automation* (ICRA 2003), vol. 3 (2003) pp. 2356–2362.
14. M. Epstein, J. E. Colgate and M. A. MacIver, "Generating Thrust with a Biologically Inspired Robotic Ribbon Fin," **In**: *Proceedings of the IEEE/RSJ International Intelligent Robots and Systems*, Piscataway, NJ (Oct. 9–15, 2006) pp. 2412–2417.
15. T. Yasuyuki, I. Hirofumi and S. Naoto, "The Motion of a Fish-Like Underwater Vehicle with Two Undulating Side Fins," *Proceedings of the 3rd International Symposium on Aero Aqua Bio-Mechanisms* (2006).
16. C. Zhou and K. H. Low, "Kinematic Modeling Framework for Biomimetic Undulatory Fin Motion Based on Coupled Nonlinear Oscillators," **In**: *Proceedings of the IEEE/RSJ International Intelligent Robots and Systems*, Tianjin, China (Oct. 18–22, 2010) pp. 934–939.
17. C. Jennie, K. Eva and K. Scott, "Source seeking for two nonholonomic models of fish locomotion," *IEEE Trans. Robotics* **25**, 1166–1176 (2009).
18. J. Z. Yu, L. Z. Liu and L. Wang, "Dynamic Modeling and Experimental Validation of Biomimetic Robotic Fish," **In**: *Proceedings of the American Control Conference*, Minneapolis, MN, USA (Jun. 14–16, 2006) pp. 4129–4134.

19. K. H. Low and A. Willy, "Biomimetic motion planning of an undulating robotic fish fin," *J. Vib. Control* **12**, 1337–1359 (2006).
20. M. A. MacIver, E. Fontaine and J. W. Burdick, "Designing future underwater vehicles: Principles and mechanisms of the weakly electric fish," *J. Oceanic Eng.* **29**, 651–659 (2004).
21. Z. Chen, S. Shatara and X. B. Tan, "Modeling of biomimetic robotic fish propelled by an ionic polymer-metal composite caudal fin," *IEEE Trans. Mechatronics* **15**(3), 448–459 (2009).
22. Z. G. Zhang, "Modeling and System Identification of Three-layer Structure Electrostatic Film Motors for a Robotic Fish," **In**: *Proceedings of the IEEE International Conference Mechatronics and Automation*, Changchun, China (Aug. 9–12, 2009) pp. 2729–2734.
23. A. A. Transeth, K. Y. Pettersen and P. Liljeback, "A survey on snake robot modeling and locomotion," *J. Robotica* **27**, 999–1015 (2009).
24. J. Y. Cheng, L. X. Zhuang and B. G. Tong, "Analysis of swimming 3D waving plate," *J. Fluid Mech.* **232**, 341–355 (1991).
25. L. J. Rosenberger and M. W. Westneat, "Functional morphology of undulatory pectoral fin locomotion in the stingray taeniura lymma (chondrichthyes: dasyatidae)," *J. Exp. Biol.* **202**, 3523–3539 (1999).
26. L. J. Shang, S. Wang and M. Tan, "Motion Control for an Underwater Robotic Fish with Two Undulating Long-Fins," **In**: *Proceedings of the Joint 48th IEEE. Conference Decision and Control and 28th Chinese Control Conference*, Shanghai, China (Dec. 16–18, 2009) pp. 6478–6483.
27. J. E. Colgate and K. M. Lynch, "Mechanics and control of swimming: A review," *IEEE J. Oceanic Eng.* **29**, 660–673 (2004).
28. S. Kelouwani and K. Agbossou, "Nonlinear model identification of wind turbine with a neural network," *IEEE Trans. Energy Convers.* **19**, 607–612 (2004).